



Universiteit
Leiden
The Netherlands

Diabetes, atherosclerosis, and stenosis by AI

Jonas, R.A.; Crabtree, T.R.; Jennings, R.S.; Marques, H.; Katz, R.J.; Chang, H.J.; ... ; Villines, T.C.

Citation

Jonas, R. A., Crabtree, T. R., Jennings, R. S., Marques, H., Katz, R. J., Chang, H. J., ... Villines, T. C. (2023). Diabetes, atherosclerosis, and stenosis by AI. *Diabetes Care*, 46(2), 416-424. doi:10.2337/dc21-1663

Version: Publisher's Version

License: [Licensed under Article 25fa Copyright Act/Law \(Amendment Taverne\)](#)

Downloaded from: <https://hdl.handle.net/1887/3729144>

Note: To cite this publication please use the final published version (if applicable).



Diabetes, Atherosclerosis, and Stenosis by AI

Diabetes Care 2023;46:416–424 | <https://doi.org/10.2337/dc21-1663>

Rebecca A. Jonas,¹ Tami R. Crabtree,² Robert S. Jennings,² Hugo Marques,³ Richard J. Katz,⁴ Hyuk-Jae Chang,⁵ Wijnand J. Stuijffzand,⁶ Alexander R. van Rosendaal,⁷ Jung Hyun Choi,⁸ Joon-Hyung Doh,⁹ Ae-Young Her,¹⁰ Bon-Kwon Koo,¹¹ Chang-Wook Nam,¹² Hyung-Bok Park,¹³ Sang-Hoon Shin,¹⁴ Jason Cole,¹⁵ Alessia Gimelli,¹⁶ Muhammad Akram Khan,¹⁷ Bin Lu,¹⁸ Yang Gao,¹⁸ Faisal Nabi,¹⁹ Ryo Nakazato,²⁰ U. Joseph Schoepf,²¹ Roel S. Driessen,⁶ Michiel J. Bom,⁶ Randall C. Thompson,²² James J. Jang,²³ Michael Ridner,²⁴ Chris Rowan,²⁵ Erick Avelar,²⁶ Philippe G n reux,²⁷ Paul Knaapen,⁶ Guus A. de Waard,⁶ Gianluca Pontone,²⁸ Daniele Andreini,²⁸ Mouaz H. Al-Mallah,¹⁹ Marco Guglielmo,²⁸ Jeroen J. Bax,⁷ James P. Earls,² James K. Min,² Andrew D. Choi,⁴ and Todd C. Villines²⁹

OBJECTIVE

This study evaluates the relationship between atherosclerotic plaque characteristics (APCs) and angiographic stenosis severity in patients with and without diabetes. Whether APCs differ based on lesion severity and diabetes status is unknown.

RESEARCH DESIGN AND METHODS

We retrospectively evaluated 303 subjects from the Computed Tomographic Evaluation of Atherosclerotic Determinants of Myocardial Ischemia (CREDENCE) trial referred for invasive coronary angiography with coronary computed tomographic angiography (CCTA) and classified lesions as obstructive ($\geq 50\%$ stenosed) or nonobstructive using blinded core laboratory analysis of quantitative coronary angiography. CCTA quantified APCs, including plaque volume (PV), calcified plaque (CP), noncalcified plaque (NCP), low-density NCP (LD-NCP), lesion length, positive remodeling (PR), high-risk plaque (HRP), and percentage of atheroma volume (PAV; PV normalized for vessel volume). The relationship between APCs, stenosis severity, and diabetes status was assessed.

RESULTS

Among the 303 patients, 95 (31.4%) had diabetes. There were 117 lesions in the cohort with diabetes, 58.1% of which were obstructive. Patients with diabetes had greater plaque burden ($P = 0.004$). Patients with diabetes and nonobstructive disease had greater PV ($P = 0.02$), PAV ($P = 0.02$), NCP ($P = 0.03$), PAV NCP ($P = 0.02$), diseased vessels ($P = 0.03$), and maximum stenosis ($P = 0.02$) than patients without diabetes with nonobstructive disease. APCs were similar between patients with diabetes with nonobstructive disease and patients without diabetes with obstructive disease. Diabetes status did not affect HRP or PR. Patients with diabetes had similar APCs in obstructive and nonobstructive lesions.

CONCLUSIONS

Patients with diabetes and nonobstructive stenosis had an association to similar APCs as patients without diabetes who had obstructive stenosis. Among patients with nonobstructive disease, patients with diabetes had more total PV and NCP.

Coronary computed tomographic angiography (CCTA) has evolved into an effective noninvasive imaging modality for detecting coronary artery disease (CAD), determining

¹Department of Internal Medicine, Thomas Jefferson University Medical Center, Philadelphia, PA

²Cleerly, Inc., New York, NY

³Faculdade de Medicina da Universidade Cat lica Portuguesa, Lisboa, Portugal

⁴The George Washington University School of Medicine & Health Sciences, Washington, DC

⁵Division of Cardiology, Severance Cardiovascular Hospital and Severance Biomedical Science Institute, Yonsei University College of Medicine, Yonsei University Health System, Seoul, South Korea

⁶Amsterdam University Medical Center, VU University Medical Center, Amsterdam, the Netherlands

⁷Department of Cardiology, Leiden University Medical Center, Amsterdam, the Netherlands

⁸Ontact Health, Inc., Seoul, South Korea

⁹Division of Cardiology, Inje University Ilsan Paik Hospital, Goyang, South Korea

¹⁰Kang Won National University Hospital, Chuncheon, South Korea

¹¹Department of Internal Medicine, Seoul National University Hospital, Seoul, South Korea

¹²Cardiovascular Center, Keimyung University Dongsan Hospital, Daegu, South Korea

¹³Division of Cardiology, Department of Internal Medicine, International St. Mary's Hospital, Catholic Kwandong University College of Medicine, Incheon, South Korea

¹⁴Division of Cardiology, Department of Internal Medicine, Ewha Women's University Seoul Hospital, Seoul, South Korea

¹⁵Mobile Cardiology Associates, Mobile, AL

plaque composition, and quantifying specific atherosclerotic plaque characteristics (APCs) (1). Studies using data from CCTA have helped to elucidate the process of atherosclerotic disease progression and have identified plaque features with prognostic value for future cardiac events (2–4). These pursuits have direct clinical application as the data from CCTA have provided clinicians with an opportunity to improve diagnoses and then optimize medical and interventional management based on the presence of adverse plaques (3,5).

Patients with diabetes are known to be at high risk for CAD and, subsequently, to suffer high mortality from major adverse cardiovascular events. It is also well established that patients with ischemia-inducing stenoses are more likely to experience adverse cardiovascular events, the risk of which might be mitigated by preemptive therapeutic intervention (6,7). While the diagnostic value of APCs is still being explored, the findings of the CREDENCE (Computed Tomographic Evaluation of Atherosclerotic Determinants of Myocardial Ischemia) trial indicate that stenosis ($\geq 50\%$) and the plaque features that comprise those stenotic lesions were strongly predictive of downstream ischemia (8). It follows that understanding the APCs that comprise the lesions of patients with diabetes may similarly enhance our understanding of cardiac ischemia in this population. Furthermore, whether there are APCs that can help distinguish lesions at high risk for ischemia in patients with diabetes is unknown. These APCs include 1) atheroma burden by plaque volume (PV); 2) plaque composition, as categorized by calcified plaque (CP), noncalcified plaque (NCP), and low-density NCP (LD-NCP); 3) arterial remodeling, categorized by positive remodeling (PR) ≥ 1.10 ; and 4) lesion length (3,9). This study used CCTA

to evaluate the relationship of APCs to coronary stenosis severity and then determine whether this relationship is affected by diabetes status.

RESEARCH DESIGN AND METHODS

Study Population

The study population comprised the derivation cohort of the CREDENCE trial (clinicaltrials.gov NCT02173275), which was a prospective, multicenter diagnostic derivation-validation controlled clinical trial recruiting stable patients from 2014 to 2017 with a locked database completed in 2018 (8) along with a detailed design manuscript (10). Eligibility criteria included referral for nonemergent invasive coronary angiography (ICA) based on the American College of Cardiology/American Heart Association clinical practice guidelines for stable ischemic heart disease. All index tests were interpreted in blinded fashion by core laboratories. The Institutional Review Board of each enrolling site approved the study protocol, and all patients provided written informed consent. Patient demographics, cardiovascular risk factors, laboratory values, and medications were prospectively collected and recorded at the time of baseline and follow-up CCTAs.

CCTA Imaging Protocols

CCTA was performed using single- or dual-source CT scanners of ≥ 64 -detector rows. Sites performed CCTA in accordance with the guidelines established by the Society of Cardiovascular Computed Tomography (SCCT) (11). Patients received nitroglycerin immediately prior to CCTA acquisition to improve image quality. β -Blockers were administered to patients who required heart rate control. Image quality for CCTA was acceptable in 99% of patients.

When impaired image quality was present due to motion, poor opacification,

beam hardening, or other artifact, only the portion of the coronary artery with poor quality was excluded from the analysis. Among the 171,195 mm of vessel length evaluated, a total of 1,861 mm of vessel length (1.09%) was excluded, with an average exclusion measuring 14.1 ± 13.9 mm.

Artificial Intelligence-Guided CCTA Analysis

CCTA studies were uploaded to Cleerly Laboratories (Cleerly, Denver, CO), a U.S. Food and Drug Administration-cleared software, validated by high performance against expert readers, ICA, and intravenous ultrasound (study currently ongoing) (12–14). This artificial intelligence (AI)-aided approach performs automated analysis of CCTA using validated convolutional neural network models, including Visual Geometry Group (VGG) 19 network, 3D U-Net, and VGG Network Variant. These models use deep learning, a process based on AI-generated patterns of recognition and adaptation that are fully AI derived. Neural networks were used for lumen wall evaluation, vessel contour determination, and plaque characterization, optimizing for phase with each vessel segment analysis (15,16).

The software begins by producing a centerline along the length of a vessel for lumen and outer vessel wall contouring. Vessels are then segmented. These segments are labeled by their position both in the coronary tree as well as their position within the proximal, middle, or distal portion of the vessel itself. The software identifies areas where plaque is present by comparing a normal proximal cross-sectional reference slide to a normal distal cross-sectional reference slide on either end of a lesion. These normal cross-sectional slides are then marked to signify a lesion's proximal and distal ends.

¹⁶Department of Imaging, Fondazione Toscana Gabriele Monasterio, Pisa, Italy

¹⁷Cardiac Center of Texas, McKinney, TX

¹⁸State Key Laboratory of Cardiovascular Disease, Fuwai Hospital, Beijing, China

¹⁹Houston Methodist Hospital, Houston, TX

²⁰Cardiovascular Center, St. Luke's International Hospital, Tokyo, Japan

²¹Medical University of South Carolina, Charleston, SC

²²St. Luke's Mid America Heart Institute, Kansas City, MO

²³Kaiser Permanente San Jose Medical Center, San Jose, CA

²⁴Heart Center Research, LLC, Huntsville, AL

²⁵Renown Heart and Vascular Institute, Reno, NV

²⁶Oconee Heart and Vascular Center at St Mary's Hospital, Athens, GA

²⁷Gagnon Cardiovascular Institute at Morristown Medical Center, Morristown, NJ

²⁸Centro Cardiologico Monzino, Istituto di Ricovero e Cura a Carattere Scientifico (IRCCS), Milan, Italy

²⁹Division of Cardiovascular Medicine, University of Virginia Health System, Charlottesville, VA

Corresponding author: Rebecca A. Jonas, rebecca.jonas@jefferson.edu

Received 10 August 2021 and accepted 14 October 2022

This article contains supplementary material online at <https://doi.org/10.2337/figshare.21341007>.

© 2023 by the American Diabetes Association. Readers may use this article as long as the work is properly cited, the use is educational and not for profit, and the work is not altered. More information is available at <https://www.diabetesjournals.org/journals/pages/license>.

The software can then calculate the lesion's length (the length of uninterrupted plaque along the length of the vessel), the total plaque burden present between the markers, and then characterize the present plaque components. Maximum stenosis is calculated by identifying the ratio of a normal cross-sectional slide with the slide that demonstrates the greatest luminal narrowing. Obstructive disease was defined by a lesion with $\geq 50\%$ luminal narrowing compared with a normal cross-sectional reference slide.

The summation of data from individual lesions provided data for the patient-level analysis. This included the patient's Coronary Artery Disease Reporting and Data System (CAD-RADS) stenosis category, a 0–100% range scale divided into standardized sextiles that designate the maximum severity of a patient's coronary artery stenosis, each with an associated guideline-oriented recommendation for management. While the CAD-RADS assessment system also incorporates an assessment of plaque burden, only stenosis grades were referenced in this study (17). Because this process is performed by the AI's deep learning neural network, no manual interaction is required from the reader (18). Only after the AI algorithm completes all operations, a quality control cardiac CT trained technician reviews the results to provide any necessary manual adjustments. All images were analyzed in a blinded manner (18,19).

AI-Guided CCTA Analysis of APCs

Coronary segments with a diameter ≥ 2 mm were included using the modified 18-segment SCCT model (20,21). This threshold was specified by the original CRENDENCE study as the minimum diameter vessel to undergo investigation with ICA (8). Each vessel segment was evaluated for the presence or absence of coronary atherosclerosis, which defined a diseased vessel. Coronary atherosclerosis was defined as any tissue structure >1 mm² within the coronary artery wall that was differentiated from the surrounding epicardial tissue, epicardial fat, or the vessel lumen itself when evaluated by ICA.

For all other segments, the following APCs were evaluated:

- Atherosclerosis: Quantitative atherosclerosis characterization was performed for

every coronary artery and its branches using an automated AI-enabled web-based software platform. PVs (mm³) were calculated for each coronary lesion and then summed to compute the total PV at the patient level. When multiple lesions, whether obstructive or non-obstructive, were present in a particular vessel length, the lesion whose measurements most closely correlated with the lesion identified on quantitative coronary angiography (QCA) interrogation was coregistered to the AI analysis. PV was categorized using Hounsfield unit (HU) ranges, with LD-NCP defined as plaques with any component on a pixel-level basis and quantified on an increment of 0.1 mm³ as <30 HU, NCP defined as HU between 30 and $+350$, and CP defined as >350 HU (22). Coronary plaque burden was normalized to vessel volume to account for variation in coronary artery volume. Plaque burden was reported as the percentage of atheroma volume (PAV), which was calculated as PV/vessel volume $\times 100\%$.

- PR: Arterial remodeling was calculated by examining the lesion diameter divided by the normal reference diameter. PR was defined as a ratio ≥ 1.10 (23).

- High-risk plaque (HRP): HRP was defined as a coronary lesion with both LD-NCP and PR (8).
- Other APCs: Lesion length was defined as the measurement of uninterrupted plaque along the length of a vessel.

QCA

QCA was performed by a blinded core laboratory using an automated edge-detection algorithm by standard approaches as previously reported (24). Angiographic percentage diameter stenosis and lumen diameters of the proximal and distal reference segments were measured.

Statistical Analysis

All statistical analyses were performed using SAS 9.4 software (SAS Institute, Cary, NC). Data for demographic and outcomes variables were tested for normality using the Shapiro-Wilk test. Continuous variables that significantly departed from normality are reported as median and first and third quartiles. Normally distributed continuous variables are reported as mean and SD, and categorical variables are presented as absolute numbers with corresponding frequencies. Demographic data were compared between patients with and without diabetes using the Student

Table 1—Baseline demographics

Variable	All (N = 303)	Without diabetes (n = 208)	With diabetes (n = 95)	P value
Age (years), mean (SD)	64.4 (10.2)	68.9 (10.5)	65.7 (9.3)	0.1508
Female sex	88 (29.0)	63 (30.3)	25 (26.3)	0.4798
BMI (kg/m ²), mean (SD)	26.3 (4.2)	26.2 (4.3)	26.7 (3.9)	0.3125
Race/ethnicity				
Black	7 (2.3)	5 (2.4)	2 (2.1)	>0.999
Asian	214 (70.6)	147 (70.7)	67 (70.5)	0.9792
American Indian	0	0	0	—
White	81 (26.7)	55 (26.4)	26 (27.4)	0.8658
Hypertension	195 (64.4)	124 (59.6)	71 (74.7)	0.0108
Dyslipidemia	135 (44.6)	86 (41.3)	49 (51.6)	0.0964
Family history	59 (19.5)	37 (17.8)	22 (23.2)	0.2735
Tobacco use	146 (48.2)	101 (48.6)	45 (47.7)	0.8476
On aspirin	182 (60.1)	118 (56.7)	64 (67.4)	0.0794
On statin	169 (55.8)	108 (51.9)	61 (64.2)	0.0457
No. of diseased vessels (QCA)				
0	128 (42.2)	90 (43.3)	38 (40.0)	0.3350
1	105 (34.7)	74 (35.6)	31 (32.6)	
2	46 (15.2)	30 (14.4)	16 (16.8)	
3 (or LM)	24 (7.9)	14 (6.7)	10 (10.5)	

Data are presented as n (%) unless indicated otherwise as mean (SD). LM, left main coronary artery.

t test for normally distributed continuous variables, the Wilcoxon rank sum test for nonnormal continuous and for ordinal variables, and the χ^2 and Fisher exact tests were used to compare the distribution of categorical variables. The per-patient analysis of APC variables was similarly analyzed. Lesion length and stenosis diameter percentage reported on a per-patient basis are calculated by taking the maximum value per lesion for each patient. The per-lesion data were analyzed using the generalized estimating equations model in order to appropriately account for the multiple measures with patients. A normalizing transform was applied to continuous data that were significantly non-normal. All summary statistics are based on nontransformed values. The interaction of diabetes and presence of obstructive disease was analyzed using a generalized estimating equations model with a main effect for diabetes and obstructive disease as well as the interaction term. The van Elteren test was used to perform a stratified analysis to account for statistically significant differences at baseline in hypertension and statin use between patients with and without diabetes and when comparing differences in PVs. *P* values are reported without an adjustment for multiplicity.

RESULTS

Baseline Demographics

Table 1 outlines the baseline demographics of the study cohort. The study cohort comprised 303 patients, 95 of whom had diabetes. Owing to the geography of high enrollment sites, 71% of the enrolled cohort was Asian. The average age was similar across the cohorts with and without diabetes (65.7 ± 9.3 vs. 68.9 ± 10.5 years; *P* = NS). The cohorts also had similar prevalence of common risk factors and therapy, with the exception of hypertension (74.7% vs. 59.6%; *P* = 0.01) and statin therapy (64.2% vs. 51.9%; *P* = 0.046), both of which were more common in patients with diabetes.

A total of 362 lesions were identified, 117 of which were observed in the cohort with diabetes. Overall, 48.3% (*n* = 175) of all lesions were obstructive, and 51.7% (*n* = 187) were nonobstructive. Among the subset with diabetes, 58.1% (*n* = 68) of the lesions were obstructive, and 41.9% (*n* = 49) were nonobstructive. There was no difference in the number of

stenotic coronary vessels observed in the two groups (*P* = NS).

Per-Patient APCs by Diabetes Status

Table 2 summarizes the CCTA analysis of APCs as a function of diabetes status. Patients with diabetes had more overall PV (490.7 mm^3 vs. 395.6 mm^3 ; *P* = 0.02) and CP (191.9 mm^3 vs. 90.7 mm^3 ; *P* = 0.03) than patients without diabetes, even after adjusting for baseline differences in hypertension and statin use. When evaluating by %PAV, patients with diabetes had greater %PAV (19.2% vs. 13.7%; *P* = 0.002), %PAV CP (7.4% vs. 3.6%; *P* = 0.01), and maximum lesion lengths (30.5 mm vs. 25.2 mm; *P* = 0.03). Diabetes status did not affect PR, HRP, the maximum number of diseased vessels, maximum stenosis, or CAD-RAD stenosis scores.

Per-Lesion APCs by Diabetes Status and Angiographic Stenosis

Table 3 reflects the quantification of APCs stratified by diabetes status and angiographic stenosis. In patients with diabetes, obstructive lesions did not have greater

PV (*P* = 0.23), lesion length (*P* = 0.11), PR (*P* = 0.63), NCP (*P* = 0.08), or LD-NCP (*P* = 0.11) than nonobstructive lesions. Patients without diabetes had greater PV (55.9 mm^3 vs. 44.2 mm^3 ; *P* = 0.049) and PAV (52.5% vs. 42.6%; *P* < 0.0001), with higher PAV NCP (32.6% vs. 25.7%; *P* = 0.03) in obstructive compared with nonobstructive lesions. Maximum lesion lengths, CAD-RADS stenosis grade, PR, and HRP showed similar patterns across obstructive and nonobstructive lesions regardless of diabetes status.

Per-Patient APCs in Patients With Diabetes With Nonobstructive Angiographic Stenoses Versus Patients Without Diabetes With Obstructive Angiographic Stenosis

Table 4 further compares APCs of patients without diabetes with obstructive stenosis to patients with diabetes and nonobstructive stenosis. This analysis reflects that despite patients without diabetes with obstructive disease having greater maximal stenosis (*P* < 0.0001), more diseased vessels, and more PR (*P* = 0.047), other APCs, including PV, NCP,

Table 2—Per-patient APCs by diabetes status

Variable	Without diabetes (<i>n</i> = 208)	With diabetes (<i>n</i> = 95)	<i>P</i> value
PV (mm^3)	395.6 (209.3, 739.6)	490.7 (321.4, 833.4)	0.0461*
LD-NCP (mm^3)	6.5 (2.3, 15.9)	7.2 (2.5, 14.1)	0.9634
NCP (mm^3)	277.7 (138.1, 501.6)	296.2 (164.5, 466.5)	0.4058
CP (mm^3)	90.7 (31.6, 263.7)	191.9 (59.7, 405.4)	0.0293*
%PAV	13.7 (8.4, 22.2)	19.2 (11.8, 28.6)	0.0024*
%PAV LD-NCP	0.20 (0.09, 0.51)	0.26 (0.10, 0.46)	0.8549
%PAV NCP	9.1 (5.4, 14.5)	10.4 (6.7, 14.0)	0.2281
%PAV CP	3.6 (1.1, 8.5)	7.4 (2.2, 13.6)	0.0086*
Remodeling index	1.30 (1.20, 1.40)	1.30 (1.20, 1.50)	0.6627
PR	178 (86.4)	80 (84.2)	0.5935
HRP	158 (76.0)	76 (80.0)	0.4368
Max lesion length (mm)	25.2 (16.5, 39.8)	30.5 (21.8, 42.3)	0.0293
Stenosis (%)	61.0 (43.0, 82.5)	63.0 (49, 100)	0.0842
CAD-RADS**	3.2 (1.3)	3.4 (1.2)	0.1533
No. of diseased vessels (QCA)			
0	90 (43.3)	38 (40.0)	0.3350
1	74 (35.6)	31 (32.6)	
2	30 (14.4)	16 (16.8)	
3 (or LM)	14 (6.7)	10 (10.5)	

Data are presented as median (quartile 1, quartile 3) or *n* (%). LM, left main coronary artery. **P* values are adjusted for hypertension and statin use. **CAD-RADS stenosis defined as 0 = 0%; 1 = 1–25%; 2 = 26–49%; 3 = 50–69%; 4 = 70–99%; 5 = 100%.

Table 3—Per-lesion APCs by diabetes status and angiographic obstructive versus nonobstructive angiographic stenosis

Variable	Without diabetes			With diabetes		
	Nonobstructive (n = 138)	Obstructive (n = 107)	P value	Nonobstructive (n = 49)	Obstructive (n = 68)	P value
PV (mm ³)	44.2 (12.7, 107.2)	55.9 (21.8, 145.3)	0.0499	37.4 (9.1, 111.9)	51.8 (14.8, 166.2)	0.2299
LD-NCP (mm ³)	0.40 (0, 1.40)	0.60 (0.10, 2.50)	0.1416	0.20 (0, 1.60)	0.20 (0, 1.10)	0.1119
NCP (mm ³)	27.1 (8.6, 66.5)	30.3 (12.4, 90.0)	0.0506	15.1 (6.8, 58.8)	25.1 (7.3, 77.2)	0.0751
CP (mm ³)	8.9 (0.70, 39.3)	10.2 (1.5, 39.9)	0.8131	12.4 (0.9, 53.3)	12.5 (3.4, 70.6)	0.3763
%PAV	42.6 (16.6)	52.5 (16.8)	<0.0001	45.4 (18.2)	52.7 (18.8)	0.0532
%PAV LD-NCP	0.37 (0, 1.02)	0.64 (0.04, 2.20)	0.09222	0.15 (0, 0.66)	0.27 (0, 1.02)	0.1114
%PAV NCP	25.7 (16.6, 35.1)	32.6 (19.2, 48.0)	0.0290	22.8 (11.9, 31.4)	26.4 (14.0, 37.9)	0.2134
%PAV CP	10.9 (1.3, 25.9)	10.2 (2.6, 25.7)	0.9587	12.4 (1.2, 32.8)	18.8 (6.1, 37.5)	0.2399
Remodeling index	1.09 (0.19)	1.06 (0.28)	0.3184	1.09 (0.24)	1.09 (0.30)	0.9593
PR, n (%)	46 (33.3)	31 (29.0)	0.0637	15 (30.6)	25 (36.8)	0.6300
HRP, n (%)	58 (42.0)	41 (38.3)	0.5812	18 (36.7)	23 (33.8)	0.6882
Lesion length (mm)	12.0 (7.5, 23.0)	12.8 (7.5, 26.0)	0.2232	11.3 (5.8, 22.3)	13.4 (7.0, 26.4)	0.1098
Stenosis (%)	32.5 (16.5)	53.7 (21.9)	<0.0001	33.7 (15.8)	51.3 (20.4)	<0.0001
CAD-RADS*	1.8 (0.7)	2.8 (1.0)	<0.0001	1.8 (0.6)	2.7 (1.0)	<0.0001

Data are presented as median (quartile 1, quartile 3) or mean (SD), unless indicated otherwise as n (%). *CAD-RADS stenosis defined as 0 = 0%; 1 = 1–25%; 2 = 26–49%; 3 = 50–69%; 4 = 70–99%; 5 = 100%.

PAV, PAV NCP, PAV LD-NCP, and lesion lengths ($P = \text{NS}$) were similar to patients with diabetes and nonobstructive stenoses (Fig. 1). Supplementary Table 1 provides a full continuum of total PVs in patients with diabetes and without diabetes stratified by obstructive disease.

APCs in Patients With Nonobstructive Angiographic Stenoses Stratified by Diabetes Status

When comparing the APCs of patients with and without diabetes with nonobstructive stenoses, CCTA analysis finds that patients with diabetes and nonobstructive disease have greater plaque burden than patients without diabetes. Patients with diabetes had more overall PV (471.6 mm³ vs. 267.3 mm³; $P = 0.02$), %PAV (14.6% vs. 10.7%; $P = 0.02$) with more diseased vessels ($P = 0.03$), and greater maximum stenosis ($P = 0.02$) and CAD-RADS stenosis severity ($P = 0.045$) than the patients without diabetes. Patients with diabetes also had greater NCP burden, with more NCP (280.1 mm³ vs. 166.6 mm³; $P = 0.03$) and PAV NCP (10.2% vs. 6.6%; $P = 0.02$), than patients without diabetes. PR and HRP were similar between groups. This analysis is provided in Supplementary Table 2.

CONCLUSIONS

In this multicenter study, we used CCTA to quantify APCs in a cohort with and without diabetes. Importantly, this study identifies several important plaque phenotypes:

First, patients with diabetes have greater PV, CP, and longer lesion lengths compared with patients without diabetes while maintaining comparable maximum stenosis and CAD-RADS stenosis grade.

Second, patients with diabetes and nonobstructive stenosis demonstrate greater plaque burden, diseased vessels, maximum stenosis, and a greater NCP burden than patients without diabetes who have nonobstructive stenosis.

Third, patients with diabetes and nonobstructive stenosis exhibit APCs similar to patients with obstructive stenosis who do not have diabetes.

Our study identified that patients with diabetes have a greater overall plaque burden with greater calcified PV compared with control subjects. While this may be explained in part by statin therapy, which has been shown to promote plaque stability through the transformation of low-attenuation plaque and NCP to CP, CP burden remains significantly greater in patients with diabetes after controlling for statin use (25–28). Prior

studies have observed that patients with diabetes have high levels of CP (29–31). The literature has also established that CP develops at faster rates in patients with diabetes and that high calcified PVs are associated with future adverse coronary events (31,32). However, the study by Wong et al. (32) presents a nuance to this association when they report that women with diabetes have a higher mortality rate from cardiovascular events but are simultaneously more likely to have a coronary artery calcium score of 0. Mrgan et al. (30) provide an explanation for this discordance when they observe that the absolute volume and ratio of NCP (specifically LD-NCP volume) to total PV has been observed to be higher in patients with diabetes, providing one explanation for increased risk for adverse cardiac events despite high levels of calcified or stable PVs. Subsequently, women were found to have higher levels of NCP (30,33). While our analysis was not stratified by sex, these insights provide a context in which to evaluate the findings of our subsequent patient analyses.

When comparing patients with nonobstructive atherosclerosis, our study shows that patients with diabetes have a greater burden of disease, with higher PV and more diseased vessels, than patients without diabetes. However, notably, there

Table 4—Per-patient APCs in patients with diabetes with nonobstructive angiographic stenoses versus patients without diabetes with obstructive angiographic stenoses

Variable	Without diabetes, obstructive (n = 118)	With diabetes, nonobstructive (n = 38)	P value
PV (mm ³)	545.0 (286.6, 866.2)	471.6 (291.3, 717.0)	0.1581
LD-NCP (mm ³)	9.7 (3.7, 18.6)	8.1 (2.6, 14.2)	0.1575**
NCP (mm ³)	333.4 (178.0, 575.1)	280.1 (135.5, 406.6)	0.0921
CP (mm ³)	130.5 (45.7, 355.2)	126.6 (12.9, 252.3)	0.2189**
% PAV	17.4 (10.9, 27.0)	14.6 (8.9, 23.9)	0.2453
% PAV LD-NCP	0.32 (0.12, 0.61)	0.27 (0.11, 0.47)	0.2729
% PAV NCP	11.5 (7.3, 16.7)	10.2 (6.6, 13.2)	0.1154
% PAV CP	4.0 (1.6, 12.1)	3.2 (0.3, 11.0)	0.3143**
Remodeling index	1.30 (1.20, 1.50)	1.30 (1.20, 1.40)	0.3396
PR	104 (88.1)	29 (76.3)	0.0465
HRP	92 (78.0)	28 (73.7)	0.5858
Max lesion length (mm)	28.8 (17.0, 41.5)	28.4 (15.0, 43.8)	0.6994
Max stenosis	75 (62.0, 100)	48.0 (39.0, 61.0)	<0.0001
Max CAD-RADS*, mean (SD)	3.9 (1.0)	2.6 (0.9)	
No. of diseased vessels (QCA)			
0	0	38 (100)	—
1	74 (62.7)		
2	30 (25.4)		
3 (or LM)	14 (11.9)		
No. of diseased vessels (CCTA)			
0	7 (5.9)	21 (55.3)	<0.0001
1	57 (48.3)	10 (26.3)	
2	29 (24.6)	6 (15.8)	
3 (or LM)	25 (21.2)	1 (2.6)	

Data are presented as median (quartile 1, quartile 2) or as n (%), unless indicated otherwise as mean (SD). LM, left main coronary artery. *CAD-RADS stenosis defined as 0 = 0%; 1 = 1–25%; 2 = 26–49%; 3 = 50–69%; 4 = 70–99%; 5 = 100%. **Inadequate power to distinguish a difference.

is also higher percentage of atheroma volume of NCP compared with control subjects. Our observation that patients with diabetes have high volumes of NCP in nonobstructive lesions compared with patients without diabetes is consistent with the wider literature that documents young patients with diabetes and early signs of CAD have a plaque profile predominated by NCP, even in instances when there is a coronary artery calcium score of 0 (29,30,34). The significance of NCP is further outlined in a review of plaque components associated with adverse coronary events by Thomsen et al. (35), where the authors show that on a patient level, CP was more commonly associated with patients with stable angina, while NCP volume was greater in patients with acute coronary syndrome. However, more recent research from a subanalysis of the SCOT-HEART (Scottish COmputed Tomography of the HEART) trial highlights the

newly acknowledged prognostic significance of a subset of NCP with low attenuation. In the SCOT-HEART subanalysis, the authors show that low-attenuation NCP burden (referred to as “low-density NCP” in this study) surpassed traditional risk scores, coronary artery calcium scoring, and stenosis severity as the strongest predictor of acute coronary syndrome (36). It consequently bears emphasis that patients with diabetes not only have a similar amount of PV but also similar NCP, PAV NCP, and PAV LD-NCP as patients without diabetes with obstructive cardiac disease.

The identification of obstructive coronary stenoses has remained central to current CAD evaluation methods and is especially important for the population with diabetes. Our study shows that individuals without diabetes have more PV, PAV, and more NCP in obstructive lesions, a profile similar to what had

been observed at the patient level as the difference between patients without and with diabetes with nonobstructive disease. On the patient level, patients without diabetes but with obstructive lesions had a similar plaque profile to patients with diabetes and nonobstructive disease, and similarly, the lesion level plaque profile for patients without diabetes is not far behind the patient-level trend. This lesion-level analysis suggests that those additional plaque components may have been incorporated into the obstructive lesions of patients without diabetes.

The composition of obstructive plaques, or late disease, in patients with diabetes provides further insight into the next stage of plaque progression. Here the data show that patients with diabetes have similar plaque composition in obstructive and nonobstructive lesions. This aligns with the findings of a prior

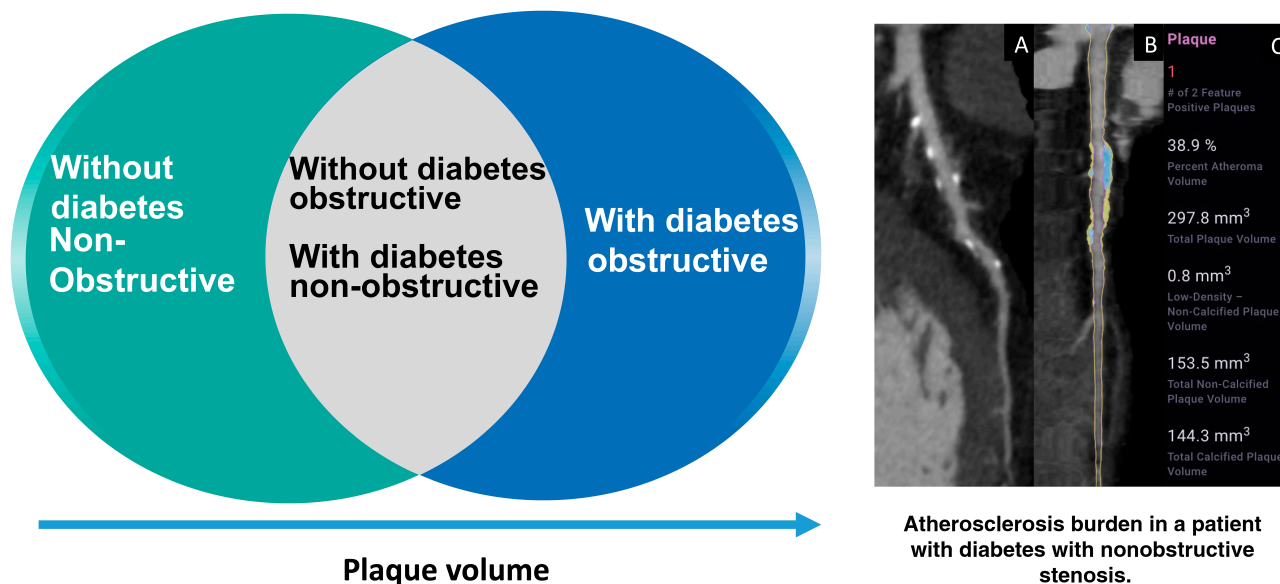


Figure 1—*Left*: Patients with diabetes with nonobstructive stenosis were associated with similar adverse plaque characteristics and PV as patients without diabetes with obstructive stenosis by AI-guided CCTA. *Right*: A 66-year-old patient with diabetes with CCTA undergoing AI-aided evaluation of stenosis and quantitative atherosclerosis burden. The patient demonstrates left anterior descending mild stenosis of 44% with a vessel-specific burden of plaque (297.8 mm³) consisting of both calcified (144.3 mm³) and noncalcified (153.5 mm³) plaque. The atheroma volume is 38.9%. In this patient, overall PV was 848.3 mm³ with overall atheroma volume of 17.8% and atheroma volume of CP of 8.6%. *A*: Shows a CCTA curved multiplanar reformat with plaque identified. *B*: Shows a straight reformat with a color overlay of NCP (yellow) and CP (blue). *C*: Shows a graphical output of the quantified PV by AI-aided evaluation.

study on age-based plaque composition that showed that the plaque profile becomes less distinct with more varied APC composition in older patients with long-standing disease (37). It also suggests that additional components other than distinct APCs and stenosis may be responsible for ischemia-inducing lesions in this population. While the combination of APCs and stenosis severity have been identified as features predictive of ischemia, a substudy of the ISCHEMIA (International Study of Comparative Health Effectiveness With Medical and Invasive Approaches) trial showed that after stratifying for stenosis, severity of CAD itself was most closely associated with acute coronary syndrome risk (7). This suggests an area of further research in which early plaque burden is incorporated into ischemia prediction to assess its prognostic value in patients with diabetes.

This study has limitations. Although the cohort evaluated was prospectively enrolled from a large, multicenter clinical trial, this evaluation is post hoc, and all study results should consequently be considered hypothesis-generating. Additionally, due to the geographic location of the study's major recruitment sites, the study cohort was ethnically homogeneous, restricting the ability to generalize findings

to the greater population. Only the validation arm of the CREDENCE study was used, resulting in small sample sizes for subanalyses. As a result, while the study was able to show that the majority of APCs were similar among patients with diabetes and nonobstructive disease and patients with obstructive disease without diabetes, the sample size was unable to achieve adequate power for the assessment of CP, PAV CP, or LD-NCP. That analysis will require a larger cohort.

Further, we evaluated coronary artery stenoses at a single point in time rather than across a longitudinal period. Coronary lesions are known to be dynamic, and how plaque composition changes as a function of worsening stenosis severity remains unknown (38).

Finally, we used angiographic coronary stenosis as a marker of CAD severity, although the long-term clinical utility of using stenosis as the primary indicator of CAD severity is unclear. To date, large-scale randomized controlled trials have not observed improved clinical outcomes from treatment of stenotic lesions, and therefore, the place of stenosis severity in disease prognostics remains uncertain (39,40). While the literature contains studies that have successfully correlated inflammatory biomarkers with APCs, these data were not collected over the course of

this trial and, consequently, will need to be pursued in future studies (33).

In this post hoc analysis of the multicenter CREDENCE study, we used CCTA evaluated by AI to quantify APCs in patients with and without diabetes and found that patients with diabetes and nonobstructive stenosis had an association to similar adverse plaque characteristics as patients without diabetes who have obstructive stenosis. These insights support ongoing study into the plaque profile of diabetic patients to assess features that may have prognostic value for adverse cardiac events in this population.

Funding. A.D.C. is supported by a grant from the GW Heart and Vascular Institute.

Duality of Interest. J.P.E., H.M., J.K.M., and A.D.C. have equity interest in Cleerly Inc. J.P.E., R.S.J., T.R.C., and J.K.M. are employees of Cleerly Inc. No other potential conflicts of interest relevant to this article were reported.

Author Contributions. R.A.J., J.P.E., R.S.J., T.R.C., J.K.M., A.D.C., and T.C.V. contributed to data analysis and interpretation of results. R.A.J., J.P.E., R.S.J., T.R.C., J.K.M., A.D.C., and T.C.V. contributed to draft manuscript preparation. J.P.E., J.K.M., and A.D.C. contributed to study conception and design. H.M., H.-J.C., J.H.C., J.-H.D., A.-Y.H., B.-K.K., C.-W.N., H.-B.P., S.-H.S., J.C., A.G., M.A.K., B.L., Y.G., F.N., R.N., U.J.S., R.S.D., M.J.B., R.C.T., J.J.J., M.R., C.R., E.A., P.G., P.K., G.A.d.W., G.P., and D.A.,

contributed to data collection. W.J.S, A.R.v.R., and J.J.B. contributed to proof revisions. All authors reviewed the results and approved the final version of the manuscript. A.D.C. is the guarantor of this work and, as such, had full access to all the data in the study and takes responsibility for the integrity of the data and the accuracy of the data analysis.

Prior Presentation. Parts of this study were presented in abstract form at the European Society of Cardiology (ESC) Congress, virtual meeting, 27–30 August 2021.

References

- Nakanishi R, Motoyama S, Leipsic J, Budoff MJ. How accurate is atherosclerosis imaging by coronary computed tomography angiography? *J Cardiovasc Comput Tomogr* 2019;13:254–260
- Williams MC, Moss AJ, Dweck M, et al. Coronary artery plaque characteristics associated with adverse outcomes in the SCOT-HEART Study. *J Am Coll Cardiol* 2019;73:291–301
- Ferencik M, Mayrhofer T, Bittner DO, et al. Use of high-risk coronary atherosclerotic plaque detection for risk stratification of patients with stable chest pain: a secondary analysis of the PROMISE Randomized Clinical Trial. *JAMA Cardiol* 2018;3:144–152
- Chang HJ, Lin FY, Lee SE, et al. Coronary atherosclerotic precursors of acute coronary syndromes. *J Am Coll Cardiol* 2018;71:2511–2522
- Williams MC, Newby DE, Nicol ED. Coronary atherosclerosis imaging by CT to improve clinical outcomes. *J Cardiovasc Comput Tomogr* 2019;13:281–287
- Hachamovitch R, Hayes SW, Friedman JD, Cohen I, Berman DS. Comparison of the short-term survival benefit associated with revascularization compared with medical therapy in patients with no prior coronary artery disease undergoing stress myocardial perfusion single photon emission computed tomography. *Circulation* 2003;107:2900–2907
- Reynolds HR, Shaw LJ, Min JK, et al. Outcomes in the ISCHEMIA trial based on coronary artery disease and ischemia severity. *Circulation* 2021;144:1024–1038
- Stuijzand WJ, van Rosendael AR, Lin FY, et al.; CRENCE Investigators. Stress myocardial perfusion imaging vs coronary computed tomographic angiography for diagnosis of invasive vessel-specific coronary physiology: predictive modeling results from the Computed Tomographic Evaluation of Atherosclerotic Determinants of Myocardial Ischemia (CRENCE) Trial. *JAMA Cardiol* 2020;5:1338–1348
- Abdelrahman KM, Chen MY, Dey AK, et al. Coronary computed tomography angiography from clinical uses to emerging technologies: JACC State-of-the-Art Review. *J Am Coll Cardiol* 2020;76:1226–1243
- Rizvi A, Hartaigh BO, Knaapen P, et al. Rationale and design of the CRENCE trial: Computed Tomographic evaluation of atherosclerotic Determinants of myocardial Ischemia. *BMC Cardiovasc Disord* 2016;16:190
- Abbara S, Blanke P, Maroules CD, et al. SCCT guidelines for the performance and acquisition of coronary computed tomographic angiography: a report of the Society of Cardiovascular Computed Tomography Guidelines Committee: endorsed by the North American Society for Cardiovascular Imaging (NASCI). *J Cardiovasc Comput Tomogr* 2016;10:435–449
- Choi AD, Marques H, Kumar V, et al. CT Evaluation by Artificial Intelligence for Atherosclerosis, Stenosis and Vascular Morphology (CLARIFY): a multi-center, international study. *J Cardiovasc Comput Tomogr* 2021;15:470–476
- Hakim D. Comparison of endothelial shear stress (ESS) computation utilizing non-invasive coronary computed tomography angiography (CCTA) vs invasive intravascular ultrasound (IVUS) Imaging. Poster presented at the American Heart Association Scientific Sessions, 13–15 November 2021, Boston, MA (and virtual experience)
- Earls JP, Choi A, Griffin WF, Marques H, Barkovich E, Riess J. Artificial intelligence evaluation of coronary stenosis on CT coronary angiography, comparison with quantitative coronary angiography; a CRENCE trial sub-study. *J Am Coll Cardiol* 2021;77(Suppl.1):1285
- Singh G, Al'Aref SJ, Van Assen M, et al. Machine learning in cardiac CT: basic concepts and contemporary data. *J Cardiovasc Comput Tomogr* 2018;12:192–201
- Carin L, Pencina MJ. On deep learning for medical image analysis. *JAMA* 2018;320:1192–1193
- Cury RC, Abbara S, Achenbach S, et al.; Endorsed by the American College of Cardiology. CAD-RADS(TM) Coronary Artery Disease - Reporting and Data System. An expert consensus document of the Society of Cardiovascular Computed Tomography (SCCT), the American College of Radiology (ACR) and the North American Society for Cardiovascular Imaging (NASCI). *J Cardiovasc Comput Tomogr* 2016;10:269–281
- U.S. Food and Drug Administration. Cleerly Labs 510 (k) premarket notification. 2019. Accessed 10 August 2021. Available from: https://www.accessdata.fda.gov/cdrh_docs/pdf19/K190868.pdf
- Hwang TJ, Kesselheim AS, Vokinger KN. Lifecycle regulation of artificial intelligence- and machine learning-based software devices in medicine. *JAMA* 2019;322:2285–2286
- Leipsic J, Abbara S, Achenbach S, et al. SCCT guidelines for the interpretation and reporting of coronary CT angiography: a report of the Society of Cardiovascular Computed Tomography Guidelines Committee. *J Cardiovasc Comput Tomogr* 2014;8:342–358
- Budoff MJ, Dowe D, Jollis JG, et al. Diagnostic performance of 64-multidetector row coronary computed tomographic angiography for evaluation of coronary artery stenosis in individuals without known coronary artery disease: results from the prospective multicenter ACCURACY (Assessment by Coronary Computed Tomographic Angiography of Individuals Undergoing Invasive Coronary Angiography) trial. *J Am Coll Cardiol* 2008;52:1724–1732
- Boogers MJ, Broersen A, van Velzen JE, et al. Automated quantification of coronary plaque with computed tomography: comparison with intravascular ultrasound using a dedicated registration algorithm for fusion-based quantification. *Eur Heart J* 2012;33:1007–1016
- Nakazato R, Shalev A, Doh JH, et al. Quantification and characterisation of coronary artery plaque volume and adverse plaque features by coronary computed tomographic angiography: a direct comparison to intravascular ultrasound. *Eur Radiol* 2013;23:2109–2117
- Danad I, Raijmakers PG, Driessen RS, et al. Comparison of coronary CT angiography, SPECT, PET, and hybrid imaging for diagnosis of ischemic heart disease determined by fractional flow reserve. *JAMA Cardiol* 2017;2:1100–1107
- Lee SE, Chang HJ, Sung JM, et al. Effects of statins on coronary atherosclerotic plaques: the PARADIGM Study. *JACC Cardiovasc Imaging* 2018;11:1475–1484
- Inoue K, Motoyama S, Sarai M, et al. Serial coronary CT angiography-verified changes in plaque characteristics as an end point: evaluation of effect of statin intervention. *JACC Cardiovasc Imaging* 2010;3:691–698
- Zeb I, Li D, Nasir K, et al. Effect of statin treatment on coronary plaque progression – a serial coronary CT angiography study. *Atherosclerosis* 2013;231:198–204
- Andelius L, Mortensen MB, Nørgaard BL, Abdulla J. Impact of statin therapy on coronary plaque burden and composition assessed by coronary computed tomographic angiography: a systematic review and meta-analysis. *Eur Heart J Cardiovasc Imaging* 2018;19:850–858
- Nezarat N, Budoff MJ, Luo Y, et al. Presence, characteristics, and volumes of coronary plaque determined by computed tomography angiography in young type 2 diabetes mellitus. *Am J Cardiol* 2017;119:1566–1571
- Mrgan M, Funck KL, Gaur S, et al. High burden of coronary atherosclerosis in patients with a new diagnosis of type 2 diabetes. *Diab Vasc Dis Res* 2017;14:468–476
- Wong ND, Nelson JC, Granston T, et al. Metabolic syndrome, diabetes, and incidence and progression of coronary calcium: the Multiethnic Study of Atherosclerosis study. *JACC Cardiovasc Imaging* 2012;5:358–366
- Wong ND, Cordola Hsu AR, Rozanski A, et al. Sex differences in coronary artery calcium and mortality from coronary heart disease, cardiovascular disease, and all causes in adults with diabetes: the Coronary Calcium Consortium. *Diabetes Care* 2020;43:2597–2606
- Mrgan M, Gram J, Hecht Olsen M, et al. Sex differences in coronary plaque composition evaluated by coronary computed tomography angiography in newly diagnosed Type 2 diabetes: association with low-grade inflammation. *Diabet Med* 2018;35:1588–1595
- Madaj PM, Budoff MJ, Li D, Tayek JA, Karlsberg RP, Karpman HL. Identification of noncalcified plaque in young persons with diabetes: an opportunity for early primary prevention of coronary artery disease identified with low-dose coronary computed tomographic angiography. *Acad Radiol* 2012;19:889–893
- Thomsen C, Abdulla J. Characteristics of high-risk coronary plaques identified by computed tomographic angiography and associated prognosis: a systematic review and meta-analysis. *Eur Heart J Cardiovasc Imaging* 2016;17:120–129
- Williams MC, Kwicinski J, Doris M, et al. Low-attenuation noncalcified plaque on coronary computed tomography angiography predicts myocardial infarction: results from the multicenter SCOT-HEART Trial (Scottish Computed Tomography of the HEART). *Circulation* 2020;141:1452–1462
- Jonas R, Earls J, Marques H, et al. Relationship of age, atherosclerosis and angiographic stenosis using artificial intelligence. *Open Heart* 2021;8:e001832

38. Ahmadi A, Leipsic J, Blankstein R, et al. Do plaques rapidly progress prior to myocardial infarction? The interplay between plaque vulnerability and progression. *Circ Res* 2015;117:99–104
39. Maron DJ, Hochman JS, Reynolds HR, et al.; ISCHEMIA Research Group. Initial invasive or conservative strategy for stable coronary disease. *N Engl J Med* 2020;382:1395–1407
40. Boden WE, O'Rourke RA, Teo KK, et al.; COURAGE Trial Research Group. Optimal medical therapy with or without PCI for stable coronary disease. *N Engl J Med* 2007;356:1503–1516